Design Interactions of AC- and DC-Side Filters for Traction Drives with SiC Inverters

Hedieh Movagharnejad, Benjamin Knebusch, Axel Mertens, Bernd Ponick
Institute for Drive Systems and Power Electronics
Leibniz University of Hannover
Hannover, Germany
Tel.: +49 / (511) – 762-14338
Fax: +49 / (511) – 762-3040
E-Mail: Hedieh.Movagharnejad@ial.uni-hannover.de, Benjamin.knebusch@ial.uni-hannover.de, Mertens@ial.uni-hannover.de, Ponick@ial.uni-hannover.de
URL: https://www.ial.uni-hannover.de

Acknowledgements

The authors gratefully acknowledge financial support from the German Federal Ministry of Education and Research (BMBF) under grant number 16EMO0252 (Project acronym: UmSiChT).

Keywords

« EMC/EMI», « Passive filters», « High frequency power converter», « High power density systems», « Electrical drive».

Abstract

This paper proposes a straightforward comprehensive design methodology for selecting and dimensioning parameters of common AC- Side filters and investigates the interactions between AC- and DC-side filters to avoid any over dimensioning in a traction drive system. A test setup has been implemented to validate the simulative investigations.

1. Introduction

Traction drives with silicon carbide (SiC) inverters offer several advantages such as lower losses and higher efficiency at partial load, increased vehicle range, higher power density and lower noise. However, the high switching frequencies related to SiC inverters - in addition to the desired switching loss reduction - also lead to steep voltage gradients (du/dt) of up to over 50 kV/µs. Possible consequences are damage to the electrical motor (winding and bearings), accelerated ageing of insulation materials due to resulting partial discharges, and electromagnetic interference (EMI) problems [1]-[5]. For these reasons, SiC components can only be used to a limited extent with today's converter and machine structures and their voltage gradients must be reduced. This significantly decreases the efficiency and associated advantages. Besides, the cost increases due to larger chip sizes.

In order to counteract the problem mentioned, the use of output AC filters, such as a du/dt filter to limit the slope of output voltages or a sine-wave filter to generate sinusoidal output voltages, can be considered. Moreover, in order to reduce the generated high frequency (HF) common-mode (CM) current and stress on the motor bearings, HF-CM chokes can be applied between the inverter output and the motor [6]-[8]. Furthermore, to suppress the EMI noise generated due to the fast variation of the switching node voltage, EMI filters are connected between the fast switching converters and the power supply [9].

This paper proposes a comprehensive design methodology for typical output AC filters and investigates the interactions of input DC and output AC filters to obtain an optimized design procedure for filter sizing in traction drive systems. This design process simultaneously considers several important parameters and selects optimal solutions with respect to size and weight.

2. Analyzed System Structure

The system, which is considered in this paper is shown in Fig. 1.

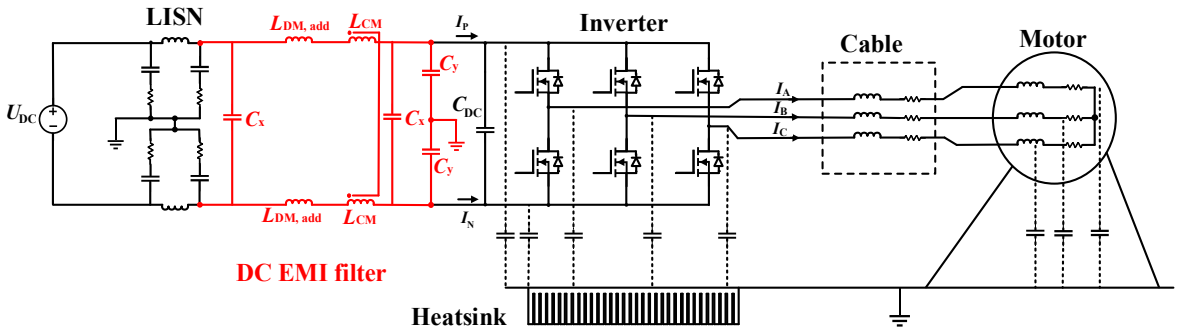

Fig. 1: Structure of the considered system

The considered system comprises a DC source, a DC line impedance stabilization network (LISN), and a three-phase inverter with SiC MOSFETs, which is connected via a cable to the induction motor. In Fig. 1, the red part belongs to the DC EMI filter, which is connected between LISN and DC side of the inverter. In [9], a comprehensive design methodology for dimensioning multi-stage DC EMI filters has been proposed. This paper focuses on the design approach for selecting an appropriate AC filter topology and its effect on the DC EMI filter design.

3. AC-Filters Design Approach

3.1. Sine-Wave Filter

Fig. 2 (a) shows an exemplary sine-wave filter, which is connected between the inverter output and the motor. The sine-wave filter, which forms a passive second-order low-pass filter, comprises a capacitor ($C_{F,s}$) to limit the steep voltage gradients, and an inductor ($L_{F,s}$) to limit the di/dt and correspondingly reduce the capacitor charging current. In this arrangement, a feedback from the capacitors' star point to the DC- Rail is considered to make a low impedance path for CM current and leading CM current into the DC- Rail. This can reduce the CM voltage at the motor terminals.

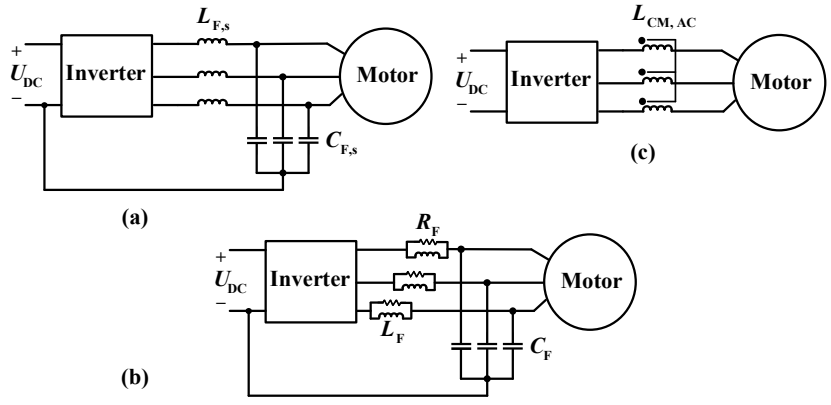

Fig. 2: AC filter topologies (a): sine-wave filter, (b): du/dt filter, (c): CM-Choke

Sine-wave filter operation depends mainly on the $L_{F,s}$ and $C_{F,s}$ values, as well as on the DC input voltage (U_{DC}) and the switching frequency (f_s). The choice of selecting filter parameters is not straightforward and depends on many important factors such as filter current ripple, desired voltage ripple on the filter output or motor terminals, a trade-off between the inductor value and thus the capacitor ripple current, losses and the size of the filter. Hence, in this paper, it is tried to propose and summarize a straightforward design procedure for selecting the filter component parameters.

Fig. 3 (left) presents a flowchart for the design of sine-wave filters. In this design methodology, with input data such as DC link voltage, switching frequency, fundamental frequency (f_0), rated output power (P_{out}), and load characteristics, the design process can be started. By designing sine-wave filters, some considerations should be made. The fundamental frequency voltage drop on the inductor should not be too large. Moreover, the cut-off frequency of the filter should be selected so that the HF noise generated will be attenuated. Furthermore, the consumed reactive power of the filter capacitors should be limited. The considered conditions are as follows:

- Fundamental frequency voltage drop across the filter < 10 % of the input voltage,
- 10* fundamental frequency < filter cut-off frequency < 0.5*switching frequency,
- Capacitors reactive power < 5 % of the inverter output power,
- Minimum inductance of the filter to be determined from maximum allowable current ripple.

Following the step-by-step design procedure, the values of $L_{F,s}$ and $C_{F,s}$ can be extracted. The size of a sine-wave filter is mainly defined by the size of its inductor. Therefore, from several valid designs, the one resulting in the smallest inductance is selected. It should be mentioned that by increasing the switching frequency, the size of the sine-wave filter can be reduced. The design input data and extracted filter parameters according to the design procedure can be found in the table in Fig. 3 (right).

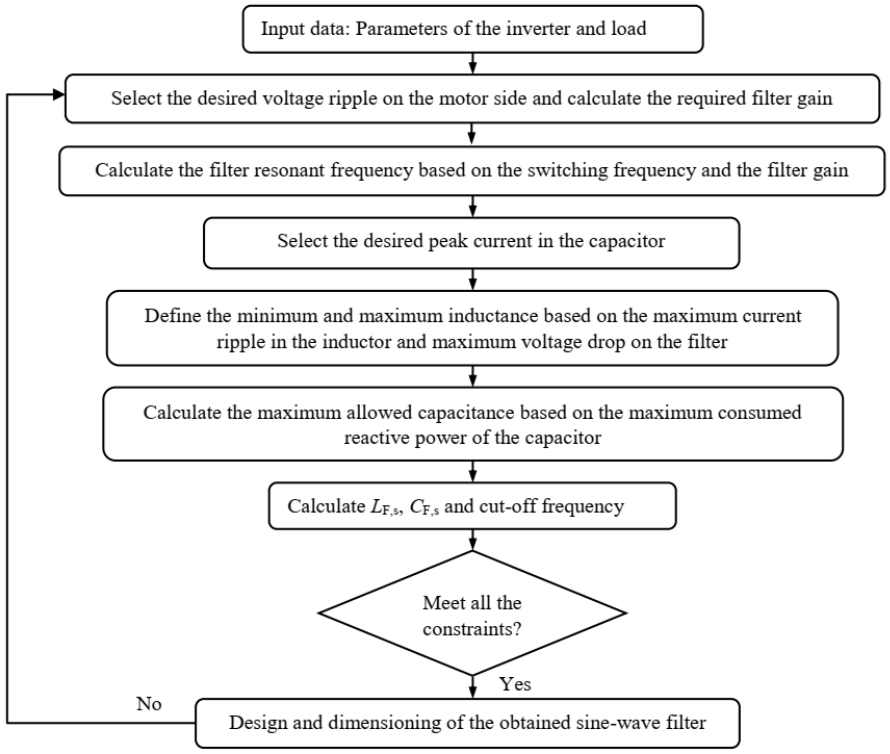

Input data
f_s = 50 kHz
f_0 = 1 kHz
U_{DC} = 600 V
P_{out} = 10 kW
I_{Load} (rms) = 15 A

Sine-wave filter parameters	
$L_{F,s}$	$C_{F,s}$
145 µH	0.6 µF

Fig. 3: Sine-wave filter design flowchart (left), Design input data and extracted sine-wave filter parameters (right)

For the conducted disturbances in the range of 150 kHz to 30 MHz, the FFT analysis of the CM and the differential mode (DM) disturbance spectrum in the frequency domain was performed. The IEC CISPR

25 standard was used to check compliance with EMI standards. Fig. 4 shows the U_{CM} interference spectrum at the LISN and the motor for the case without and with a sine-wave filter. It should be mentioned that the AC sine-wave filter does not influence the DC side DM voltage, since the DC and AC sides are decoupled due to the DC link capacitor. The simulations have been done at U_{DC} = 600 V and f_s = 50 kHz. Considering the U_{CM} disturbance spectrum at the LISN, it is clear that adding a sine-wave filter on the AC side with DC feedback can significantly reduce the disturbance at the LISN especially in the lower frequency range, which can notably reduce the demand for DC EMI filter. Based on the DC EMI filter design methodology proposed in [9], the required L_{CM} for the one-stage DC EMI filter is around 4.3 mH for the case without any AC filter, and this value reduces significantly to 154 µH if the aforementioned sine-wave filter is added to the AC side. Hence, it is recommendable to design a sine-wave filter in the system before the DC EMI filter design to avoid over-dimensioning of the DC side EMI filter. Moreover, a remarkable CM noise reduction can be detected at the motor terminals.

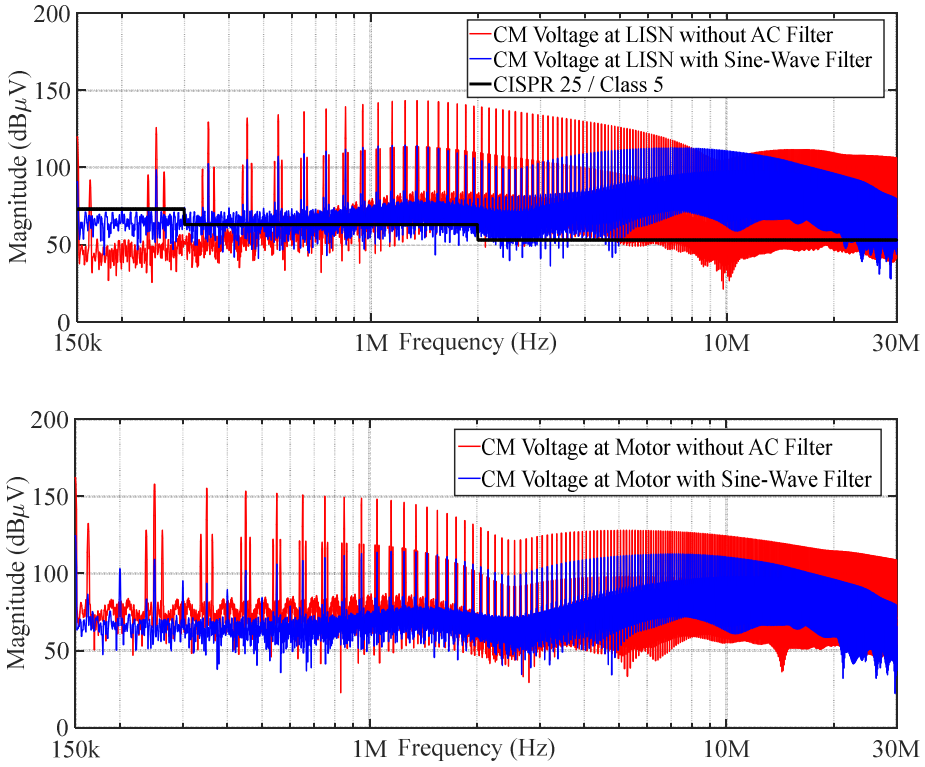

Fig. 4: Simulation results at U_{DC} = 600 V, f_s = 50 kHz, n = 0/min; U_{CM} at LISN and motor: without and with sine-wave filter

3.2. du/dt Filter

Another option for an AC filter is a du/dt filter, which comprises also an additional damping resistor, and can be seen in Fig. 2 (b). du/dt filters are passive second-order low-pass filters, and the frequency response can be adjusted by selecting the inductance L_F and the capacitance C_F. The filter resonant frequency is selected to be higher than the switching frequency. The energy of the resonance oscillation between L_F and C_F is dissipated in the damping resistors R_F. In order to design a du/dt filter, a design methodology has been considered mainly based on [7], which starts with listing of all available values for R_F, L_F and C_F and formation of all permutations of components. After this, a systematic limiting process of component parameters will be performed by some conditions, as follows:

- C_F > effective capacitance of the motor: In order to ensure the filtering effect during the operation of an electrical machine, the filter must provide a lower impedance path for the HF noise signals than the electrical machine. To achieve this, C_F must be larger than the effective capacitance of the motor.

- Desired du/dt at the filter output and filter time constant (τ) calculation: $\tau_{linear} = 0.8\frac{U_{DC}}{du/dt}$ & $\tau = \sqrt{L_F C_F}$. After that, the selection can be limited by $\tau_{linear} < \tau < 1.5 * \tau_{linear}$.
- Damping degree: $D > 1$: Other permutations can be eliminated, which cannot meet the requirement $D = \frac{1}{2R_F}\sqrt{\frac{L_F}{C_F}}$.

Consequently, possible component values will be determined and the expected du/dt from their step responses can be achieved and further limitations can be done if the solutions do not meet the requirements. Moreover, power dissipation in the damping resistors can be calculated (losses per phase: $P_{R,avg} = C_F . U_{DC}^2 . f_s$) and the permutations with the least total volume and power losses will be chosen. The losses, which should be dissipated by the resistors, are linearly dependent on the switching frequency. Although the components required to implement a du/dt filter are very small compared to the sine-wave filter, it should be mentioned that resistors with higher power dissipation are required for each increase in the switching frequency. Here, a du/dt of 12 V/ns at the filter output was considered as a condition for the investigations. Table 1 shows the best possible combination results that enable the requirements to be met at U_{DC} = 600 V and f_s = 50 kHz.

Table 1: Extracted du/dt filter parameters

at U_{DC} = 600 V, f_s = 50 kHz	L_F = 2 µH	C_F = 1.5 nF	R_F = 16 Ω	D = 1.1

To investigate the interaction of du/dt filters on the DC side, the U_{CM} interference spectrum has been plotted at the LISN and the motor (Fig. 5).

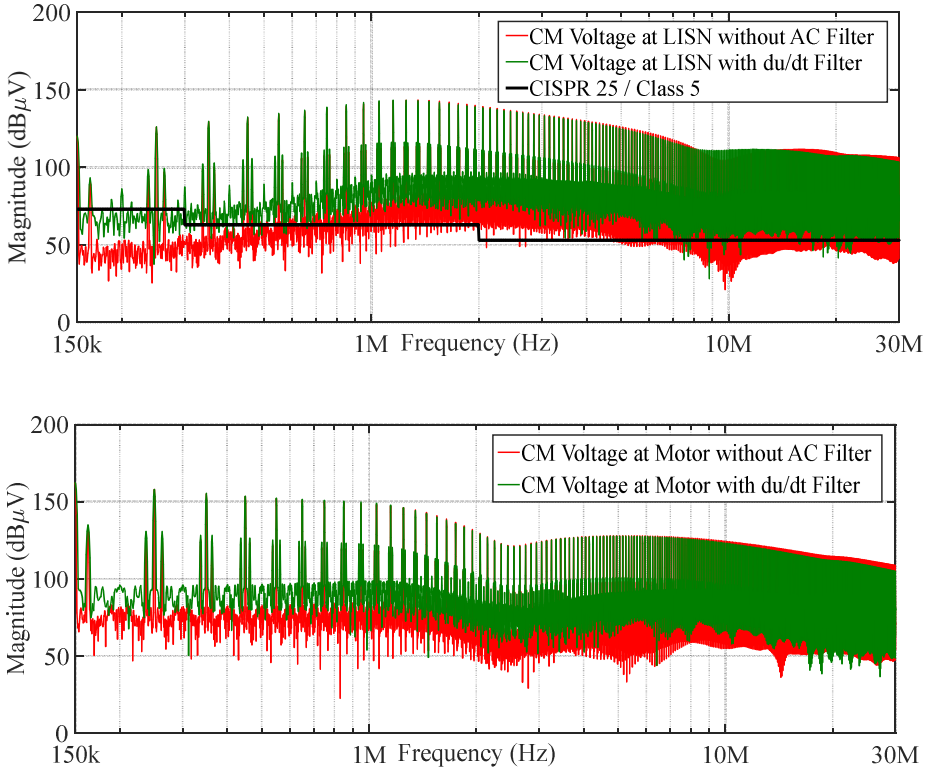

Fig. 5: Simulation results at U_{DC} = 600 V, f_s = 50 kHz, n = 0/min; U_{CM} at LISN and motor: without and with du/dt filter

It can be seen from the results that the presence of a du/dt filter does not affect the DC side EMI filter requirement, as it shows its effect only on the interference reduction in the HF range (MHz range).

This can be seen also in the results at the motor terminals. The insertion of a du/dt filter between the inverter and the motor can effectively decelerate the steep voltage edges but does not affect the EMI disturbances much.

3.3. CM-Choke

Another type of AC filter that can be considered is a CM core (Fig. 2 (c)). AC CM cores are placed over the line power cables between the inverter output and the motor input. In this configuration, the cores operate as a CM-choke. These types of cores are provided to reduce the HF CM current and correspondingly lower the stress on the motor bearings. Moreover, there is no fundamental frequency voltage drop across the chokes. It should be mentioned that these cores do not eliminate switching frequency noise.
In order to select an appropriate CM core and the corresponding required inductance value of the CM-choke, it is recommendable to investigate the whole system in simulations, to observe the peak CM currents at the motor terminals, and to define how much this CM current should be reduced. Then, the approximate value for the CM-choke inductance can be extracted, and based on this value and expected saturation characteristics of the materials, as well as core dimensions, an appropriate core can be chosen and inserted into the system.

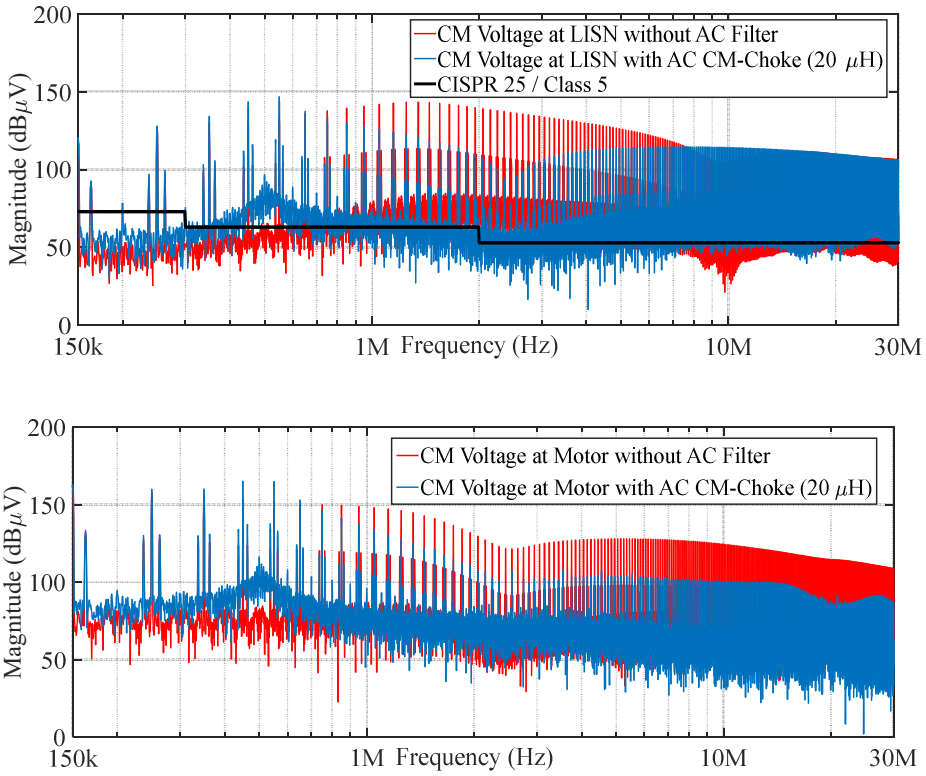

Fig. 6: Simulation results at U_{DC} = 600 V, f_s = 50 kHz, n = 0/min; U_{CM} at LISN and motor: without and with AC CM-choke

Fig. 6 shows the simulation results for the case without and with AC CM-choke. In this investigation, a CM inductance of $L_{CM,AC}$ = 20 µH has been chosen. By insertion of this CM-choke, a notable reduction in the CM current at the motor terminals can be seen (Fig. 7). The CM current reduces from its maximum value of 19.5 A to 6.5 A if $L_{CM,AC}$ = 20 µH is added. Besides, it can be seen from the CM voltage spectrum at the LISN, that there is no effective reduction in the CM noise in the low frequency range. But it should be mentioned that by inserting higher values of $L_{CM,AC}$, the LISN side CM voltage spectrum can be reduced remarkably and correspondingly the DC EMI filter design requirements can be affected. Hence, it is recommendable to design an AC CM-choke before the DC side EMI filter to avoid any over-

dimensioning. In addition, a notable reduction of the CM noise spectrum in the MHz region can be detected at the motor terminals.

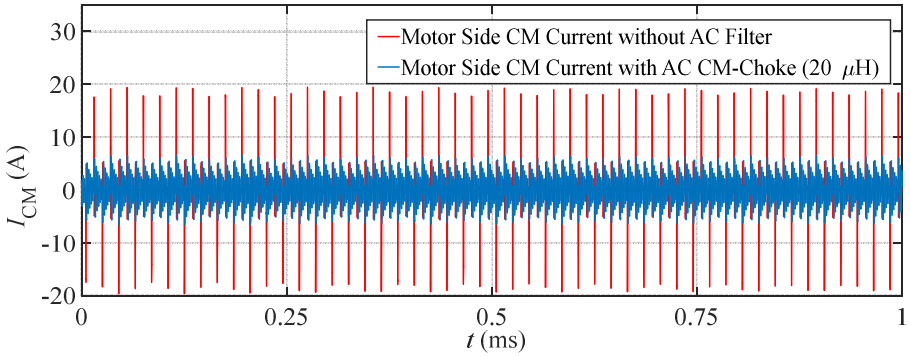

Fig. 7: Simulated I_{CM} at the motor terminals (U_{DC} = 600 V, f_s = 50 kHz, n = 0/min)

Table 2 shows a summary of the design interactions between DC EMI filter and various AC-side filters and their features.

Table 2: Design Interactions between DC- and AC-Side Filters

AC-side filter topology	Influence on DC-side EMI filter requirement	Feature
Sine-wave filter	+++	Safely inhibits du/dt, over voltages and bearing currents
du/dt filter	No influence	Reduces du/dt, but strongly affects efficiency
CM-choke	+	Reduces CM currents effectively

4. Test Setup

In order to validate the simulation results, a test setup was built as a 10 kW demonstrator. The setup (Fig. 8) consists of DC voltage source, LISN, 10 kW inverter with SiC-MOSFET half-bridge modules, and induction motor. The setup uses the Institute for Drive Systems and Power Electronics' (IAL) ControlCube, which incorporates a Xilinx Zynq 7000 (SoC) with an ARM Dual Core Cortex A9 and an Artix-7 FPGA as programmable logic (PL).

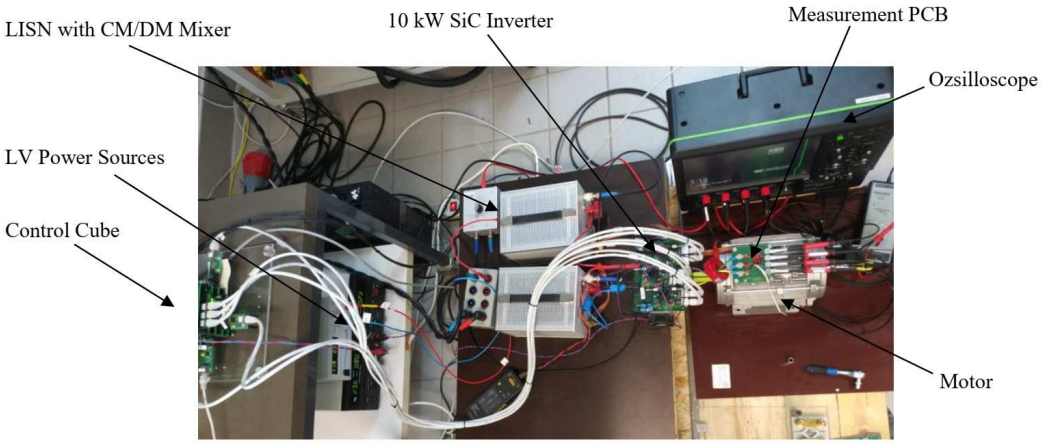

Fig. 8: Test bench setup

Fig. 9 represents the measurement results, driven at U_{DC} = 600 V, f_s = 20 kHz and n = 0/min. Fig. 9 (top) shows the U_{CM} interference spectrum at the LISN for the case without any AC filter and for the case with a du/dt filter. Here, the du/dt filter is implemented based on the design parameters of Table 1.

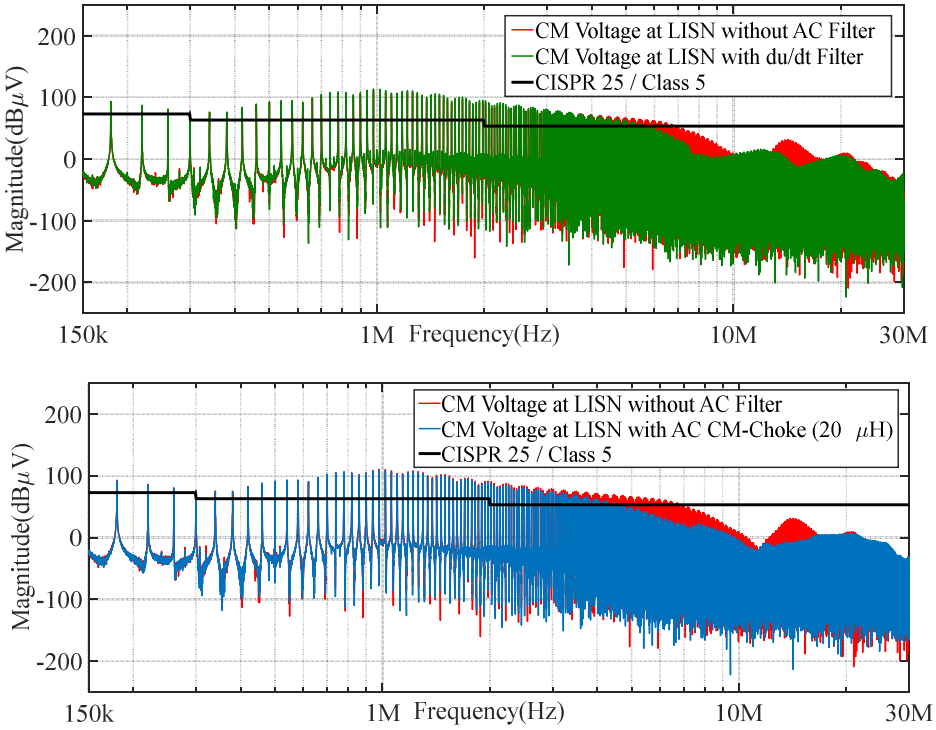

Fig. 9: Measurement results at U_{DC} = 600 V, f_s = 20 kHz, n = 0/min; U_{CM} at LISN: without and with du/dt filter (top), without and with AC CM-choke ($L_{CM,AC}$ = 20 µH) (bottom)

As it was expected, it can be seen that an insertion of a du/dt filter does not affect the U_{CM} interference spectrum in the low frequency range, and thus does not influence the DC-side EMI filter design. A reduction can be seen in the spectrum from 4 MHz. Moreover, Fig. 9 (bottom) shows the same results for the case without and with an AC-side CM-choke. Here, two CM-cores (inductance at 10 kHz: 10 µH) in series are inserted between the inverter output and the motor input. A small reduction - also in the lower frequency range - can be detected in the interference spectrum after adding the AC CM-chokes. Insertion of such cores can affect the DC-side EMI filter design depending on how large the CM-choke inductance is.

Fig. 10 and Fig. 11 represent the transient waveforms for two cases, namely the case with n = 0/min and the case with n = 1000/min. Each group of graphs present the case without any filter, the case with a du/dt filter and the case with an AC CM-choke of 20 µH between the inverter output and the motor input. In these results, phase to ground voltages ($u_{U\_GND}(t)$, $u_{V\_GND}(t)$, $u_{W\_GND}(t)$), $u_{CM}(t)$, motor star point to ground voltage ($u_{SP\_GND}(t)$) and $i_{CM}(t)$ at the motor terminals are shown. Besides, the CM voltage at the LISN $u_{CM\_LISN}(t)$ can also be seen. For each group of the results, the absolute peak values of the related waveforms can be seen in the corresponding tables.

In the case n = 0/min, where the maximum CM current occurs, it can be seen from the results that inserting an AC CM-choke has reduced the CM current from its maximum value of 6.9 A to 2.5 A. Adding an AC CM-choke is more effective compared to a du/dt filter in both, I_{CM} and U_{CM} reduction. The maximum I_{CM} value at the motor is 3.7 A, in case a du/dt filter is added.

Looking at Fig. 11, it can be seen that the maximum I_{CM} value decreases to 2.8 A for the case without any filter at n = 1000/min. Both du/dt filter and CM-choke reduce this I_{CM} value to 1.6 and 1.5 A accordingly. No remarkable reduction in the CM voltage has been detected in this condition for various AC filter cases.

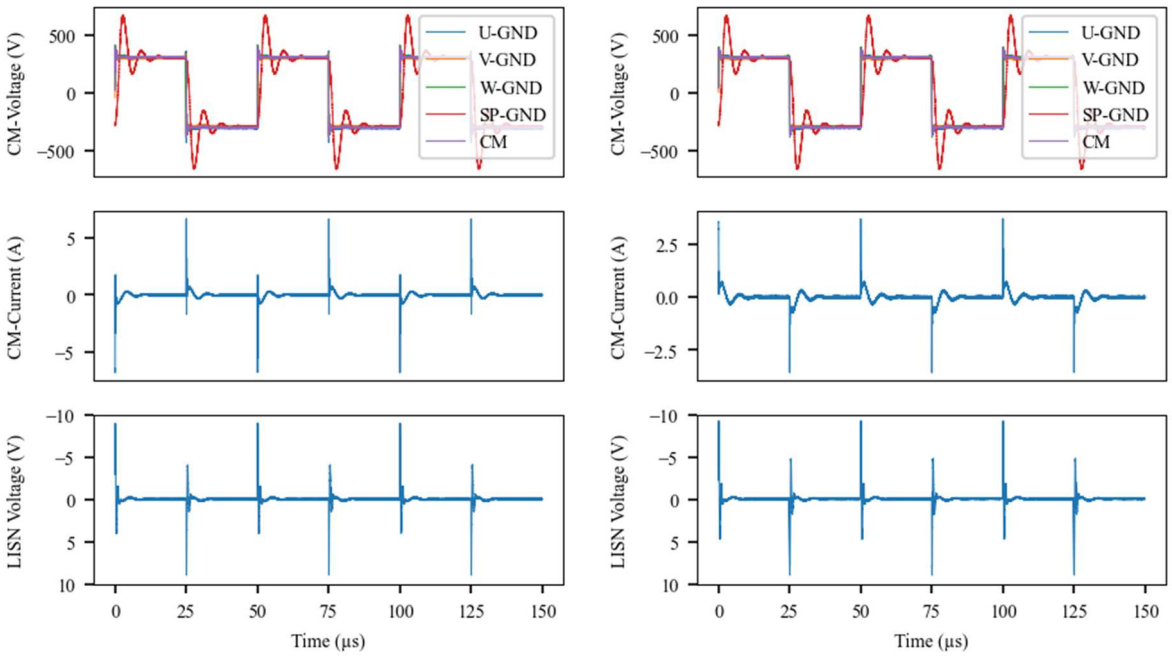

(a) (b)

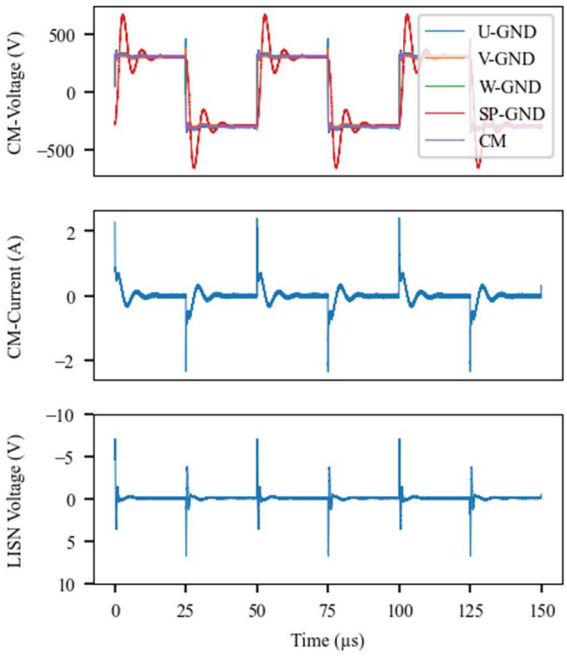

(c)

Absolute peak values of the related waveforms

	Without Filter	With du/dt Filter	With AC-CMC
$U_{CM,\,max}$	402.9 V	384.7 V	348.3 V
$U_{SP\_GND,\,max}$	674.8 V	675.2 V	675.6 V
$I_{CM,\,max}$	6.9 A	3.7 A	2.5 A
$U_{CM\_LISN,\,max}$	9.1 V	9.3 V	7.1 V

Fig. 10: Measurement results at U_{DC} = 600 V, f_s = 20 kHz, n = 0/min: without AC-filter (a), with du/dt filter (b), with AC CM-choke ($L_{CM,AC}$ = 20 µH) (c)

5. Summary and Conclusion

In this paper, a systematic design methodology for selecting and dimensioning AC-side filters for traction drive systems is proposed. Moreover, the design interactions of AC- and DC-side filters are investigated and a design priority is advised. This straightforward design process can be useful for designers to avoid over-dimensioning and to achieve an optimum filter design with a higher power density. It can be concluded that adding an AC-side filter can affect the DC-side filter design and considerations should be taken before. From the investigations, it can be concluded that adding an AC-side sine-wave filter affects the DC EMI filter design in a positive way and can help to have smaller DC

filter dimensions. Moreover, by generating sinusoidal output voltages at the motor terminals, the steep voltage gradients, over voltages and bearing currents will be inhibited safely. A du/dt filter - due to its effect in the high-frequency range - does not influence the DC EMI filter design, but reduces the steep du/dt effectively at the motor terminals. du/dt filters are not an interesting option at higher switching frequencies because of the high losses, which must be dissipated by the resistors. In addition, inserting an AC CM-choke can reduce the CM currents at the motor terminals effectively and, depending on the CM-choke inductance value, the DC-side EMI filter design can be affected in a positive way. A test setup has been implemented which validates the simulative investigations and the results comply with the simulation results.

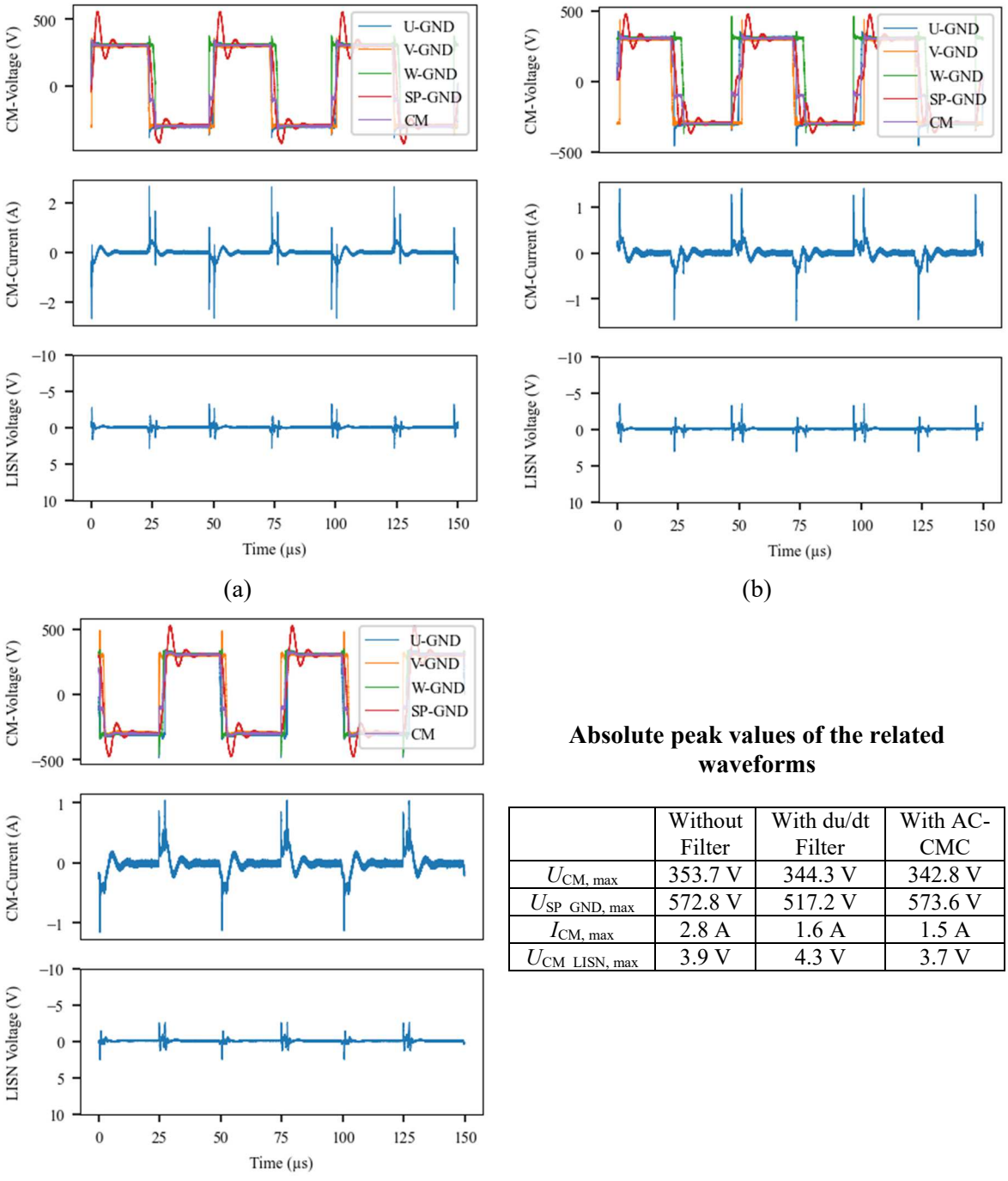

Absolute peak values of the related waveforms

	Without Filter	With du/dt Filter	With AC-CMC
$U_{CM,\,max}$	353.7 V	344.3 V	342.8 V
$U_{SP\ GND,\,max}$	572.8 V	517.2 V	573.6 V
$I_{CM,\,max}$	2.8 A	1.6 A	1.5 A
$U_{CM\ LISN,\,max}$	3.9 V	4.3 V	3.7 V

Fig. 11: Measurement results at U_{DC} = 600 V, f_s = 20 kHz, n = 1000/min: without AC-filter (a), with du/dt filter (b), with AC CM-choke ($L_{CM,AC}$ = 20 µH) (c)

References

[1] A. Mütze, “Bearing Currents in Inverter-Fed AC Motors,” Ph.D. dissertation, Technische Universität Darmstadt, 2004.
[2] H. Tischmacher, S. Gattermann, M. Kriese and E. Wittek, “Bearing wear caused by converter-induced bearing currents,” *IECON 2010 - 36th Annual Conference on IEEE Industrial Electronics Society*, pp. 784-791, 2010.
[3] M. Kriese, E. Wittek, S. Gattermann, H. Tischmacher, G. Poll, and B. Ponick, “Influence of bearing currents on the bearing lifetime for converter driven machines,” *International Conference on Electrical Machines*, pp. 1735-1739, 2012.
[4] A. Hoffmann and B. Ponick, “Method for the Prediction of the Potential Distribution in Electrical Machine Windings Under Pulse Voltage Stress,” *IEEE Transactions on Energy Conversion*, vol. 36, no. 2, pp. 1180–1187, Jun. 2021.
[5] M. Ali, J.-K. Müller, J. Friebe, and A. Mertens, “Analysis of switching performance and EMI emission of SiC inverters under the influence of parasitic elements and mutual couplings of the power modules,” *22nd European Conference on Power Electronics and Applications (EPE'20 ECCE Europe)*, 2020.
[6] N. Hanigovszki, J. Landkildehus and F. Blaabjerg, “Output filters for AC adjustable speed drives,” *APEC 07 - Twenty-Second Annual IEEE Applied Power Electronics Conference and Exposition*, Anaheim, CA, USA, 2007.
[7] J.-K. Müller, “Untersuchungen zu Ausgangsfiltern in Siliziumcarbid-Antriebswechselrichtern,” Ph.D. dissertation, Leibniz Universität Hannover, TEWISS Verlag ISBN 978-3-95900-525-8, 2021.
[8] J.-K. Müller, T. Brinker, J. Friebe and A. Mertens, “Output dv/dt filter design and characterization for a 10 kW SiC inverter,” *IECON 2018 - 44th Annual Conference of the IEEE Industrial Electronics Society*, pp. 2122-2127, 2018.
[9] H. Movagharnejad and A. Mertens, “Design methodology for dimensioning EMI filters for traction drives with SiC inverters,” *23rd European Conference on Power Electronics and Applications (EPE'21 ECCE Europe)*, 2021.